

# Antituberculosis nanodelivery system with controlled-release properties based on para-amino salicylate–zinc aluminum-layered double-hydroxide nanocomposites

Bullo Saifullah<sup>1</sup>  
Mohd Zobir Hussein<sup>1</sup>  
Samer Hasan Hussein-Al-Ali<sup>2</sup>  
Palanisamy Arulselvan<sup>3</sup>  
Sharida Fakurazi<sup>3,4</sup>

<sup>1</sup>Materials Synthesis and Characterization Laboratory, <sup>2</sup>Laboratory of Molecular Biomedicine, <sup>3</sup>Laboratory of Vaccines and Immunotherapeutics, <sup>4</sup>Department of Human Anatomy, Universiti Putra Malaysia, Serdang, Selangor, Malaysia

**Abstract:** We report the intercalation and characterization of para-amino salicylic acid (PASA) into zinc/aluminum-layered double hydroxides (ZLDHs) by two methods, direct and indirect, to form nanocomposites: PASA nanocomposite prepared by a direct method (PASA-D) and PASA nanocomposite prepared by an indirect method (PASA-I). Powder X-ray diffraction, Fourier-transform infrared spectroscopy, and thermogravimetric analysis revealed that the PASA drugs were accommodated within the ZLDH interlayers. The anions of the drug were accommodated as an alternate monolayer (along the long-axis orientation) between ZLDH interlayers. Drug loading was estimated to be 22.8% and 16.6% for PASA-D and PASA-I, respectively. The in vitro release properties of the drug were investigated in physiological simulated phosphate-buffered saline solution of pH 7.4 and 4.8. The release followed the pseudo-second-order model for both nanocomposites. Cell viability (3-[4,5-dimethylthiazol-2-yl]-2,5-diphenyltetrazolium bromide [MTT] assays) was assessed against normal human lung fibroblast MRC-5 and 3T3 mouse fibroblast cells at 24, 48, and 72 hours. The results showed that the nanocomposite formulations did not possess any cytotoxicity, at least up to 72 hours.

**Keywords:** drug-delivery system, slow-release nanocarrier, tuberculosis, biocompatible nanocomposites

## Introduction

Layered double hydroxides (LDHs) have a hydrotalcite-like structure in which some of the divalent cations are replaced by trivalent cations, which results in positively charged brucite-like sheets stacked on top of one another, resulting in a layered structure. The positive charge of these brucite-like nanosheets is neutralized by the anions and water molecules.<sup>1</sup> A variety of anions can be accommodated between the layers to counter balance the positive charge and this tendency makes them versatile to be used for different applications. The anions can be inorganic, like halides, nitrates, and sulfates, and organic, like drugs, amino acids, dyes, polymers, and DNA etc.<sup>1,2</sup> LDHs are represented by the general formula  $(M^{II}_{1-x}M^{III}_x[OH]_2)(A_{x/n}^{n-}) \cdot yH_2O$ , in which  $M^{II}$  is a divalent metal ion,  $M^{III}$  is a trivalent metal ion, and anions are used to neutralize the positive charge of the sheets. The LDHs have many applications, such as their use for extraction of toxic waste from water,<sup>3</sup> in catalysis,<sup>4</sup> and as a flame retardant,<sup>5</sup> and they have also been used in chiral separation.<sup>6</sup> Recently, the most important application of LDHs has been investigated, particularly slow-release drug-delivery systems. Different drugs have been intercalated recently into nanosheets of LDHs, such as anticancer drugs, antihistamines, antidiabetics, and antimicrobials.<sup>7,8</sup>

Correspondence: Mohd Zobir Hussein  
Materials Synthesis and Characterization  
Laboratory (MSCL), Institute of Advanced  
Technology (ITMA), Universiti Putra  
Malaysia, Serdang, Selangor 43400,  
Malaysia  
Tel +60 3 8946 6801  
Fax +60 3 8943 5380  
Email mzobir@putra.upm.edu.my

The sustained release of the intercalated anions is a tremendous characteristic of LDHs, and is supposed to enhance the therapeutic effects of the drugs. The sustained release can also increase the water solubility of the poorly soluble drugs, which ultimately reduces the side effects of the drugs related to poor water solubility. Low cytotoxicity and ease of LDH preparation make them a suitable candidate for drug-delivery purposes.

Ryu et al<sup>9</sup> applied LDHs to the antimicrobial agent cefazolin and conducted in vitro antibacterial studies. They found that the cefazolin-LDH formulation possessed higher antibacterial activity compared to naked cefazolin.<sup>9</sup> Hesse et al recently implanted ciprofloxacin-LDHs in the middle ear of rabbits infected with *Pseudomonas aeruginosa*, and clinical and microbial examination results showed the ciprofloxacin-LDHs possessed sound antimicrobial activity.<sup>10</sup>

Tuberculosis (TB) is an infectious disease caused by the bacteria *Mycobacterium tuberculosis*. The treatment duration of TB can last from 3 to 24 months, depending on the type of TB.<sup>11</sup> According to the latest facts and figures on TB in the *Global Tuberculosis Report 2012*, there were about 8.7 million new cases of TB in 2011, and 1.4 million humans lost their lives. TB is one of the top killers of women, with 300,000 deaths among HIV-negative women and 200,000 deaths among HIV-positive women in 2011.<sup>12</sup>

Para-amino salicylic acid (PASA) is an antituberculosis agent. PASA was found to be active against TB, and was used in clinical trials more than six decades ago – in 1948.<sup>13</sup> Initially, it was included in the treatment of drug-susceptible TB, but because of such side effects as anorexia, epigastric distress, nausea, vomiting, and abdominal cramps it is no longer used for drug-susceptible TB, but is still used for multidrug-resistant TB. A controlled-release formulation of PASA would be very useful for overcoming these side effects.<sup>14</sup> Different approaches are being developed for efficient and effective drug-delivery systems for the targeted and sustained release of anti-TB drugs, such as plant proteins, inhalable microparticles of polylactic acid, glucan particles and mannitol microparticles. A comprehensive review by Saifullah et al<sup>11</sup> discusses many of these delivery systems in detail.

In this article, we report the successful intercalation of PASA into the galleries of zinc/aluminum-layered double hydroxide (ZLDH) with coprecipitation and ion-exchange methods. We also studied the spatial orientation of the drug between the inorganic interlayers, the sustained-release properties, and the kinetics of its release. Furthermore, we investigated the thermal stability of the drug outside and within

inorganic interlayers of ZLDH, and we also determined the morphology of resulting nanocomposites. The main objective of this research was drug-delivery applications of these nanocomposites; therefore, we investigated cytotoxic studies on the 3T3 fibroblast mouse cell line and normal human lung cell lines where TB bacteria usually reside.

## Materials and methods

All the chemicals used were of analytical reagent grade without any further purification. PASA (99% pure), zinc nitrate hexahydrate, and aluminum nitrate nonahydrate were purchased from Sigma-Aldrich (St Louis, MO, USA). Dimethyl sulfoxide (DMSO) with 0.1% water content, used as a solvent, was purchased from Thermo Fisher Scientific (Ajax Finechem; Sydney, NSW, Australia).

### Preparation of Zn/Al-NO<sub>3</sub> LDH

A zinc to aluminum solution with a molar ratio of 4:1 was dissolved in 250 mL deionized water and stirred for 15 minutes, and the pH of the solution was raised to 7.0 by adding 2 M NaOH solution. The experiment was conducted under continuous nitrogen flux. Then, the sample was subjected to oil bath-agitation for 18 hours and then washed with deionized water three times and centrifuged.

### Preparation of nanocomposite by coprecipitation method

The sample was prepared by the method reported previously by Crepaldi et al.<sup>15</sup> Zinc nitrate hexahydrated and aluminum nitrate nonahydrated salts were dissolved in 50 mL deionized water at a molar ratio of 4:1. The solution was stirred for 15 minutes, then 0.4 M PASA prepared in 50 mL DMSO and deionized water in a molar ratio of 1:1 was added dropwise to the salt solution. Then, the pH of the solution was increased to 7.25 by dropwise addition of 0.5 M NaOH aqueous solution under a nitrogen atmosphere. After that, the sample was subjected to agitation in an oil bath at 70°C for 18 hours. Then, the sample was centrifuged and washed with deionized water. The resulting nanocomposite was denoted as PASA-D (PASA nanocomposite prepared by direct method).

### Preparation of nanocomposite by ion exchange method

The sample was prepared by adopting the method reported by Lakraimi et al.<sup>16</sup> Zinc and aluminum salts at a molar ratio of 1:4 required for 100 mL volume were dissolved in 50 mL deionized water and stirred for 15 minutes. The salt solution was added dropwise to a 250 mL beaker containing 50 mL

deionized water. NaOH 1 M solution was simultaneously added to maintain the pH at 7.00. Then, a 0.4 M solution of PASA prepared earlier in DMSO and water at a molar ratio of 1:1 in 50 mL prepared earlier was added to the freshly prepared ZLDH. The solution pH was maintained at 7.00 by simultaneous addition of 1 M NaOH solution. The whole experiment was conducted under a nitrogen atmosphere. The resulting nanocomposite was denoted as PASA-I (PASA nanocomposite prepared by an indirect method).

## Controlled-release study

The release of the drug was studied in human body-simulated buffer solutions – 0.1 M at two different pHs, 4.8 and 7.4 – to see the release profiles of PASA from the interlayer galleries of ZLDHs. There are different kinds of anions present in phosphate-buffered saline (PBS), such as mono phosphate  $\text{H}_2\text{PO}_4^-$ , dibasic phosphate  $\text{HPO}_4^{2-}$ , and  $\text{Cl}^-$ . About 0.4 mg of the nanocomposites of PASA-D and PASA-I were placed into 3.5 mL of either a pH 4.8 or pH 7.4 PBS. Maximum absorbance of 268 nm was selected in an ultraviolet-visible (UV-vis) absorption spectrophotometer. This was to compare the release of the drug from PASA-D and PASA-I in different physiological environments.

## Cell culture

3T3 mouse fibroblast cells and human lung fibroblast MRC-5 cells were obtained from the American Type Culture Collection (Manassas, VA, USA), and the cells were cultured in Dulbecco's Modified Eagle's Medium (DMEM) and Roswell Park Memorial Institute 1640 media containing 10% fetal bovine serum. Growth media contained 100 units/mL penicillin and 50  $\mu\text{g}/\text{mL}$  streptomycin. Fibroblast cells were maintained at 37°C in a humidified atmosphere of 5%  $\text{CO}_2$  in air.

## Cell viability assays

Healthy cells were seeded onto 96-well culture plates at  $1 \times 10^4$  cells per well and allowed to adhere overnight at 37°C. Then, cultured cells were incubated with medium (100  $\mu\text{L}$ ) containing dispersed LDH nanocomposites in various concentration ranges from 0.781  $\mu\text{g}/\text{mL}$  to 50  $\mu\text{g}/\text{mL}$ . The control cells were not exposed to the nanocomposites. At specific time points of 24, 48, and 72 hours of incubation, the growth medium was removed from 96-well plates and incubated with 100  $\mu\text{L}$  of the MTT (3-(4,5-dimethylthiazol-2-yl)-2,5-diphenyltetrazolium bromide) reagent in DMEM for another 3–4 hours at 37°C. The number of viable cells was analyzed by uptake of MTT, and read at 570 nm by an enzyme-linked

immunosorbent assay plate reader. Cell viability results are presented as means  $\pm$  standard deviation.

## Characterization

The X-ray diffraction (XRD) studies were done using a Shimadzu (Kyoto, Japan) XRD-6000 diffractometer. Radiation,  $\text{CuK}_\alpha$  at 30 KV and 30 mA for recording the powder XRD patterns in the range of 2–60°. Fourier-transform infrared (FTIR) spectra of the materials were recorded over the range of 4,000–400  $\text{cm}^{-1}$  on a PerkinElmer (Waltham, MA, USA) 100 series spectrophotometer by direct sample method. For the analysis of carbon, hydrogen, nitrogen, and sulfur (CHNS), a LECO (St Joseph, MI, USA) CHNS-932 instrument was used. For the thermogravimetric and differential thermogravimetric analyses, a Mettler-Toledo (Greifensee, Switzerland) instrument was used. The morphology of the sample surface was studied with a JEOL (Tokyo, Japan) JSM-6400 scanning electron microscope (SEM). For optical properties, and controlled-release studies, a Shimadzu 1650 series UV-vis spectrophotometer was utilized. Inductively coupled plasma (ICP) was used to determine  $\text{Zn}^{2+}$  and  $\text{Al}^{3+}$  concentration.

## Results and discussion

### Powder X-ray diffraction

Figure 1 shows XRD patterns for the resulting nanocomposites synthesized by coprecipitation and ion-exchange methods, labeled as PASA-D and PASA-I, respectively. The ZLDHs with nitrate anion as counter ion have been reported to have basal spacing of 8.9 Å in XRD patterns.<sup>18</sup>

The XRD patterns show that the basal spacings of the resulting nanocomposites PASA-D and PASA-I increased from 8.9 Å to 15.9 Å and 16.8 Å, respectively. The increase in basal spacing is direct evidence of successful intercalation of drug molecules in the ZLDH interlayers. The expansion is attributed to the intercalation of PASA in its anionic form inside the interlamellae of ZLDH.

Furthermore, a small amount of  $\text{CO}_3^{2-}$  coexisted between the ZLDH interlayers, partly because it is difficult to avoid contamination from the air completely and partly due to the favorable lattice stabilization enthalpy associated with the small and highly charged  $\text{CO}_3^{2-}$  anions.<sup>19</sup> The intense sharp peaks of PASA-D suggest that the nanocomposite possessed high degree crystallinity. The high crystallinity of PASA-D may be attributed to its long range and well-ordered arrangement of PASA anions in the inorganic interlamellar domain of the nanocomposite, and most probably this was taking place during the aging process. During coprecipitation, possibly better interactions took place between the negatively charged

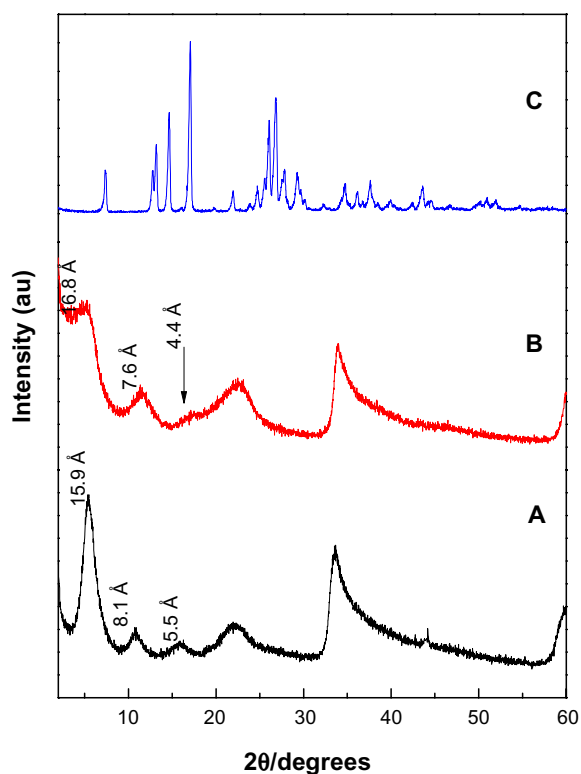


**Figure 1** X-ray diffraction patterns of PASA-D (A), PASA-I (B) and free PASA (C). **Abbreviations:** PASA, para-amino salicylic acid; PASA-D, PASA nanocomposite prepared by direct method; PASA-I, PASA nanocomposite prepared by indirect method.

PASA anions with the positively charged ZLDH inorganic layers.<sup>20</sup> In the case of the PASA-I (Figure 1B), XRD peaks were wider instead of sharp, some of the *hkl* reflections were missing, and the XRD reflections were less intense. This suggests that the nanocomposite has a lower degree of

crystallinity compared to host LDHs.<sup>16</sup> The possible reason for lower crystallinity may be the preparation method, as the host has to be rearranged during the ion-exchange process. The difference in *d*-spacing of PASA-D and PASA-I nanocomposites may be due to the layer-charge density or content of water between the layers.<sup>21</sup>

## Orientation of PASA in the inorganic interlayers of ZLDH

According to XRD analysis, the interlayer distance ( $d_{003}$ ) increased to 15.9 Å for PASA-D and 16.8 Å for PASA-I nanocomposites. The thickness of the Zn/Al-LDH layer was 4.8 Å,<sup>2</sup> thus the gallery height of Zn/Al-LDH after intercalation can be calculated by the interlayer distance minus the thickness of the Zn/Al-LDH layer, which is 11.1 Å (15.9–4.8) and 12.0 Å (16.8–4.8) for PASA-D and PASA-I nanocomposites, respectively. The long axis, short axis, and molecular thickness of PASA were calculated using ChemOffice software, and they were found to be 9.4, 7.1, and 2.9 Å, respectively (Figure 2A).

The gallery height of the PASA-D nanocomposite was 11.1 Å, which is near the value of the long axis (9.4 Å); similar is the case of the PASA-I nanocomposite, which had 12.0 Å gallery height. This result suggests that PASA anions are accommodated as an alternate monolayer (along the long-axis orientation) between layers with the carboxyl of adjacent anions attaching to the upper hydroxide layers and the amino group attached to another layer through water molecules (Figure 2B).

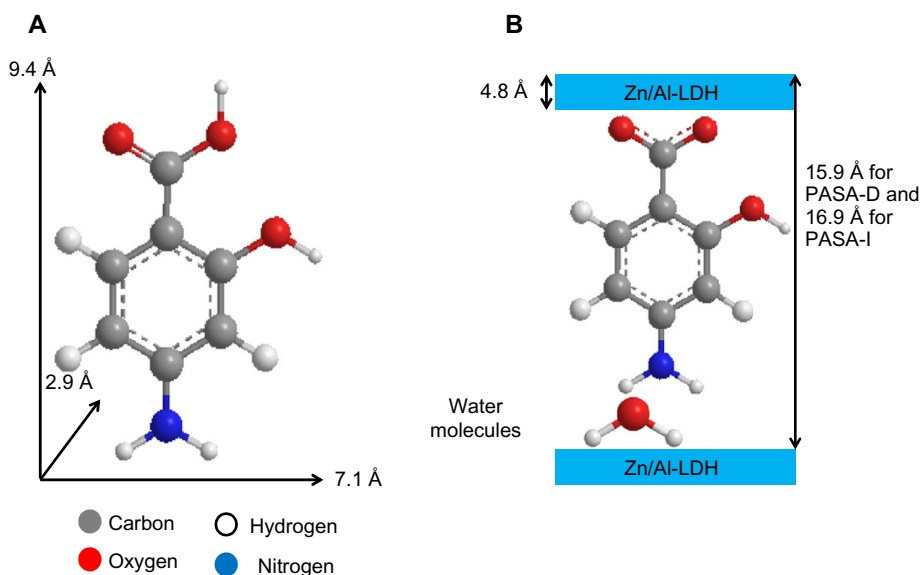


**Figure 2** Three-dimensional structure of PASA (A) and molecular structural models of PASA intercalated between interlayers of Zn/Al-LDH (B). **Abbreviations:** PASA, para-amino salicylic acid; PASA-D, PASA nanocomposite prepared by direct method; PASA-I, PASA nanocomposite prepared by indirect method; Zn/Al-LDH, zinc/aluminum-layered double hydroxide.



## Infrared spectroscopy

The intercalation of PASA anions into the interlayers of ZLDH was further confirmed by FTIR spectroscopy (Figure 3). All the vibrational bands of the PASA anions are observed together with the absorption bands of ZLDH.

The FTIR spectrum of PASA shows many absorption bands (Figure 3A). In addition to bands at high wave-number values, due to stretching of O–H, =C–H, and N–H moieties,<sup>22</sup> a band was recorded at 1,609 cm<sup>-1</sup>, due to C=O stretching of the carboxylic acid group. Due to C–C stretching of the aromatic ring, bands were recorded at 1,519 and 1,437 cm<sup>-1</sup>,<sup>22</sup> those due to the stretching mode of C–O and O–H bending of the acid and alcohol functions were recorded at 1,296 cm<sup>-1</sup> and 1,220 cm<sup>-1</sup>, respectively, while in-plane and out-of-plane of C–H bending vibrations were recorded at 1,109 and 813 cm<sup>-1</sup>, respectively.<sup>22,23</sup> A vibrations at 972 cm<sup>-1</sup> was due to the ring-breathing mode.<sup>24</sup>

The FTIR spectra recorded after intercalation of the PASA into the interlayers of ZLDH are shown in Figure 3B and C. The FTIR spectra of PASA-D and PASA-I nanocomposites contained both the characteristic peaks of pure PASA and the typical peak of ZLDH, which indicates that the PASA anions have been intercalated into the interlayer galleries of the ZLDH. Due to the negative charge of the acid group, the band of carboxylic acid (COOH) for free PASA at 1,609 cm<sup>-1</sup>

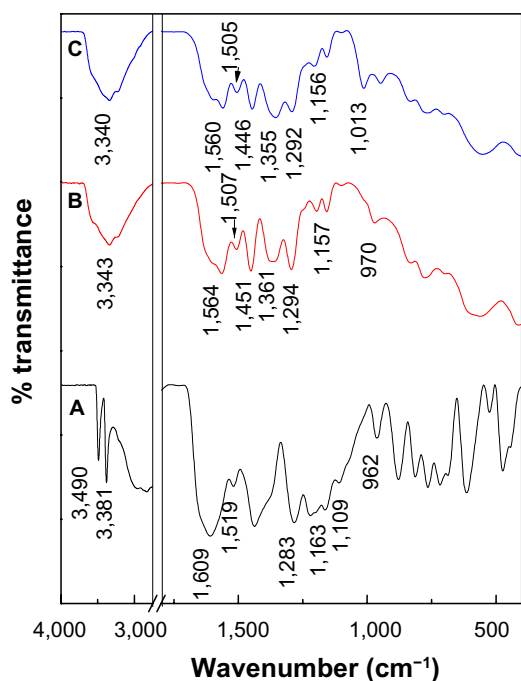


**Figure 3** Fourier-transform infrared spectra of (A) PASA, (B) PASA-D, and (C) PASA-I.

**Abbreviations:** PASA, para-amino salicylic acid; PASA-D, PASA nanocomposite prepared by direct method; PASA-I, PASA nanocomposite prepared by indirect method.

had disappeared, while new bands were recorded at 1,564 and 1,361 cm<sup>-1</sup> for the PASA-D nanocomposite, which corresponds to the asymmetric and symmetric vibrations, respectively, of the carboxylate group COO<sup>-</sup>.<sup>25</sup> In addition, bands at 1,560 and 1,355 cm<sup>-1</sup> for PASA-I nanocomposite can be observed, which corresponds to the asymmetry and symmetry, respectively, of the carboxylate group COO<sup>-</sup>.<sup>25</sup> The band assigned to the nitrate group (1,384 cm<sup>-1</sup>) was absent from both nanocomposites, and this result supported the view that the NO<sub>3</sub><sup>-</sup> anion was fully replaced by the drug. The bands below 600 cm<sup>-1</sup> are due to metal–oxygen bond-stretching modes in the inorganic layers.<sup>17,26</sup> The rest of the FTIR spectra for PASA, PASA-D, and PASA-I nanocomposite bands are listed in Table 1.

## Elemental analysis

Elemental analysis was used to determine the PASA and inorganic composition of PASA-D and PASA-I nanocomposites. As predicted, PASA-D and PASA-I nanocomposites showed the presence of both PASA and ZLDH inorganic layer constituents. This result indicated that intercalation had occurred in which PASA was already intercalated into the ZLDH interlayers.

Table 2 shows the Zn<sup>2+</sup>/Al<sup>3+</sup> molar ratios in PASA-D and PASA-I were 3.8 and 4.1, respectively, compared to 4.0 for the initial molar ratio that was prepared for the mother liquor. The C:N ratio of PASA was 6.2. In addition, the C:N ratios for PASA-D and PASA-I nanocomposites were larger than expected (9.2 and 11.3, respectively). According to FTIR spectra of PASA-D and PASA-I, strong bands at 1,361 and 1,355 cm<sup>-1</sup> are due to carbonate and COO<sup>-</sup> symmetric stretching vibration. This result indicates that a trace amount of carbonate was present in the interlamellae space of the LDH. From the elemental chemical analysis results,

**Table 1** Assignments of FTIR absorption bands of free PASA, PASA-D and PASA-I nanocomposites

Assignments	Free PASA	PASA-D	PASA-I
v (O–H) and v (N–H)	3,490, 3,381	3,343 in the layer; H <sub>2</sub> O	3,340
v (COOH)	1,609	–	–
v (C–C)	1,519, 1,437	1,507, 1,451	1,505, 1,446
δ (O–H) in plane	1,283, 1,163	1,294, 1,157	1,292, 1,156
δ (C–H) in plane	1,109	1,090	1,090
Ring-breathing mode	962	972	1,012
v <sub>as</sub> (COO <sup>-</sup> )	–	1,564	1,560
v <sub>s</sub> (COO <sup>-</sup> )	–	1,361	1,355

**Abbreviations:** PASA, para-amino salicylic acid; PASA-D, PASA nanocomposite prepared by direct method; PASA-I, PASA nanocomposite prepared by indirect method; FTIR, fourier transform infrared spectroscopy.

**Table 2** Chemical compositions of PASA, PASA-D, and PASA-I nanocomposites

Samples	Zn% <sup>a</sup>	Al% <sup>a</sup>	C% <sup>b</sup>	N% <sup>b</sup>	C/N	Drug%	Zn <sup>2+</sup> /Al <sup>3+</sup>	X
PASA	–	–	51.7	8.3	6.2	–	–	–
PASA-D	37.9	4.2	19.4	2.1	9.2	22.8 <sup>c</sup>	3.8	0.21
PASA-I	37.9	3.8	16.9	1.5	11.3	16.6 <sup>c</sup>	4.1	0.19

**Notes:** <sup>a</sup>Calculated from ICP data; <sup>b</sup>calculated from CHNS data; <sup>c</sup>calculated from UV data.

**Abbreviations:** PASA, para-amino salicylic acid; PASA-D, PASA nanocomposite prepared by direct method; PASA-I, PASA nanocomposite prepared by indirect method; UV, ultraviolet; CHNS, carbon, hydrogen, nitrogen, and sulfur; ICP, inductively coupled plasma; X, aluminium mole fraction.

the empirical formulas for PASA-I and PASA-D were found to be  $[Zn_{0.81}Al_{0.19}(OH)_2](ASA)_{0.16}(CO_3^{2-})_{0.03} \cdot xH_2O$  and  $[Zn_{0.79}Al_{0.21}(OH)_2](ASA)_{0.17}(CO_3^{2-})_{0.04} \cdot xH_2O$ , respectively.

## Thermal analysis

The thermal behavior of the PASA, PASA-D, and PASA-I nanocomposites were examined by thermogravimetric and differential thermogravimetric analysis. The thermograms are shown in Figure 4A–C. For free drug (Figure 4A), two

major thermal events occurred. The first was observed in the region of 101°C–150°C, and a sharp peak was observed at 145°C, with a 31.4% weight loss corresponding to the dehydration of PASA. The second event showed a strong peak at 227°C with 67.7% weight loss between the region of 151°C–235°C corresponding to the combustion of PASA.<sup>27</sup> Thermal behaviors of PASA-D and PASA-I nanocomposites are shown in Figure 4B and C, respectively. Three events were observed in both PASA-D and PASA-I nanocomposites. The first stage of the event in PASA-D occurred at 67°C with the weight loss of 5.6% because of the physically absorbed water on the surface of the nanocomposite, while the same event occurred in PASA-I at 75°C with a weight loss of 12.5%. The second event occurred at a temperature of 254°C with weight loss of 22.1% in the case of PASA-D, whereas the same event occurred at a temperature of 240°C with weight loss of 21.1% in the case of PASA-I. This event in both nanocomposites was due to the dehydroxylation of inorganic layers and thermal decomposition of PASA.

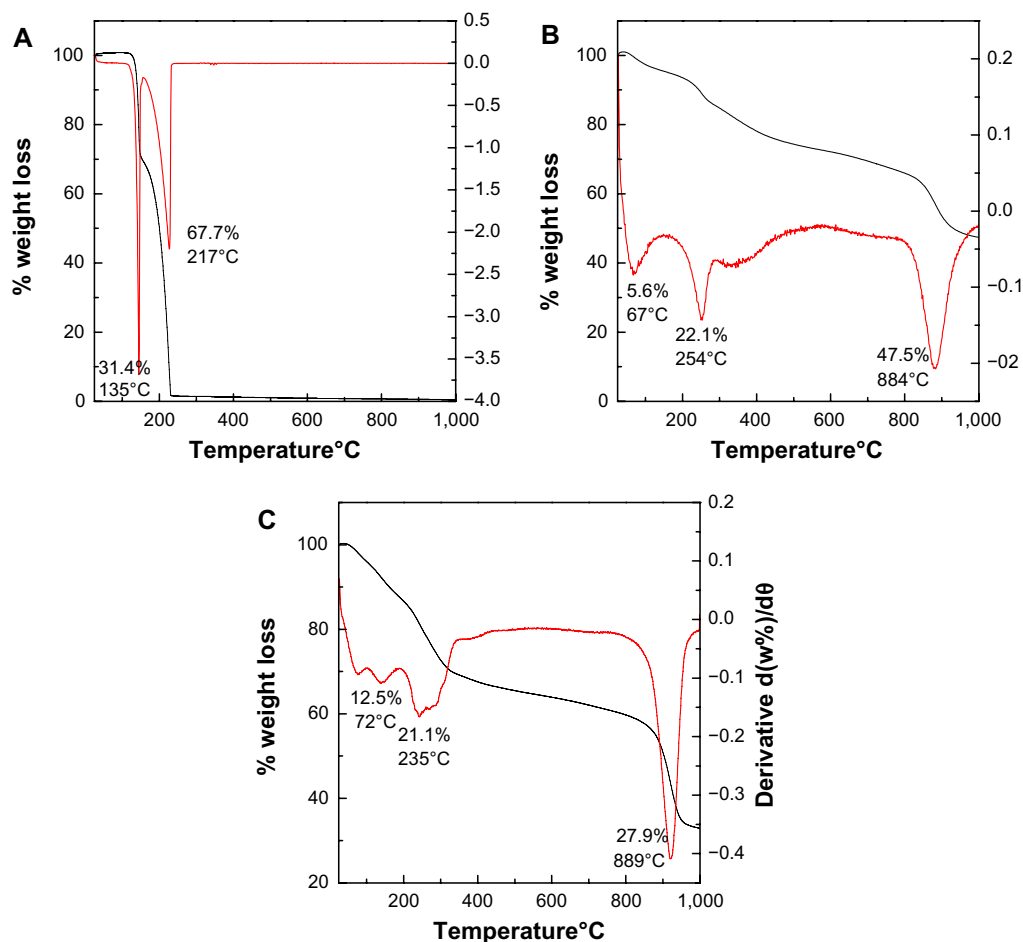


**Figure 4** Thermogravimetric analysis–differential thermogravimetric thermograms of PASA (A), PASA-D (B), and PASA-I (C).

**Abbreviations:** PASA, para-amino salicylic acid; PASA-D, PASA nanocomposite prepared by direct method; PASA-I, PASA nanocomposite prepared by indirect method.

The third event occurred at a temperature of 884°C with weight loss of 47.5% in the case of PASA-D and at a temperature of 920°C with weight loss of 28% in the case of PASA-I, due to the formation of the spinel ( $\text{ZnAl}_2\text{O}_4$ ) phase.<sup>28</sup>

The thermal stability of PASA was enhanced after intercalation into the ZLDH, as the drug decomposition occurred at 254°C in the case of PASA-D and at 240°C in the case of PASA-I, instead of 227°C. This enhanced thermal stability of PASA can be attributed to the electrostatic interaction between PASA and the inorganic interlayers of ZLDH.

## Surface morphology

The surface morphology of PASA-D and PASA-I is shown in Figure 5A–D. The micrographs were obtained using an SEM at 50,000× magnifications (A and C) and 100,000× magnifications (B and D). The SEM images for both PASA-D and PASA-I nanocomposites show agglomerates of nonporous, flaky structure without any specific shapes.

## In vitro PASA release from PASA-D and PASA-I nanocomposites

The in vitro release properties of the drug were investigated by adding the PASA-D and PASA-I nanocomposites to PBS solutions at pH 7.4 and 4.8. Figure 6A and B shows the release profiles of PASA-D and PASA-I nanocomposites in PBS solutions at pH 7.4 and 4.8. For these nanocomposites, the

first aliquot revealed a high amount of anion release (burst effect).<sup>29</sup> This probably occurred due to the release of the PASA anions adsorbed on the surface of ZLDH. The release behaviors at pH 4.8 were very fast compared to pH 7.4, which can be attributed to the partial dissolution of the ZLDH layer at acidic solutions<sup>30,31</sup> as well as the ion-exchange process. The release of PASA-D and PASA-I nanocomposites was 100% and 93%, respectively. Time taken for the release was found to be 5,400 and 8,369 minutes for PASA-D and PASA-I nanocomposites, respectively. The PASA-D and PASA-I nanocomposites were more stable at pH 7.4, as the release followed the ion-exchange process between the intercalated anions in the interlayer and phosphate anions in the buffer solutions.<sup>32</sup> The release of the drug anions at pH 7.4 in PASA-D and PASA-I nanocomposites reached 88% and 57% respectively, within 8,627 and 1,200 minutes. This was probably due to the characteristics of the ion-exchange process that occurs,<sup>16,33,34</sup> ie, this is an equilibrium process and the interlayer anions cannot be exchanged completely, unless the released organic species were removed or consumed continuously.

## Release kinetics of PASA from PASA-D and PASA-I nanocomposites

The kinetic models for the PASA release from PASA-D and PASA-I nanocomposites were analyzed using pseudo-first-order, pseudo-second-order, and parabolic diffusion kinetic equations.

The pseudo-first-order kinetic equation may be represented in a linear form as<sup>35</sup>:

$$\ln(q_e - q_t) = \ln q_e - k_1 t \quad (1)$$

where  $q_e$  and  $q_t$  are the equilibrium release amount and the release amount at any time ( $t$ ), respectively. The  $k_1$  value can be obtained from the slope by plotting  $\ln(q_e - q_t)$  versus  $t$ . The pseudo-second-order kinetic equation may be represented in a linear form as<sup>36</sup>:

$$t/q_t = 1/k_2 q_e^2 + t/q_e \quad (2)$$

The parabolic diffusion kinetic equation may be represented as<sup>37</sup>:

$$(1 - M_t/M_0)/t = k_t^{-0.5} + b \quad (3)$$

where,  $M_0$  and  $M_t$  are the drug content remaining in the ZLDH at release time 0 and  $t$ , respectively, and  $b$  is a constant.

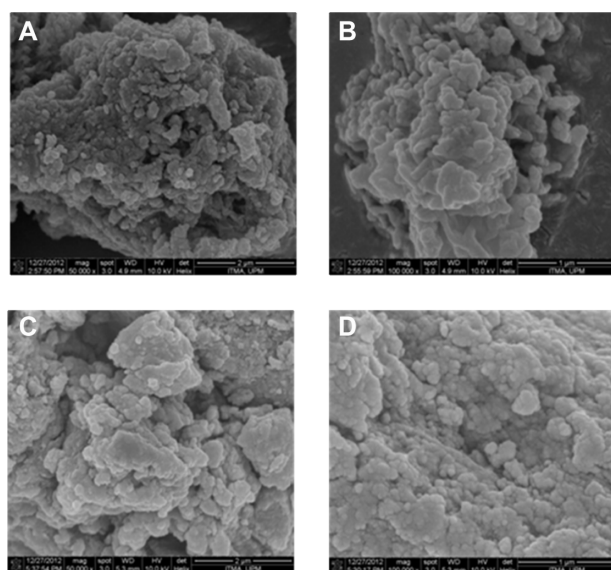


**Figure 5** Field-emission scanning electron micrographs of PASA-D (A and B) and PASA-I (C and D) nanocomposites at 50,000× and 100,000× magnifications.

**Abbreviations:** PASA, para-amino salicylic acid; PASA-D, PASA nanocomposite prepared by direct method; PASA-I, PASA nanocomposite prepared by indirect method.

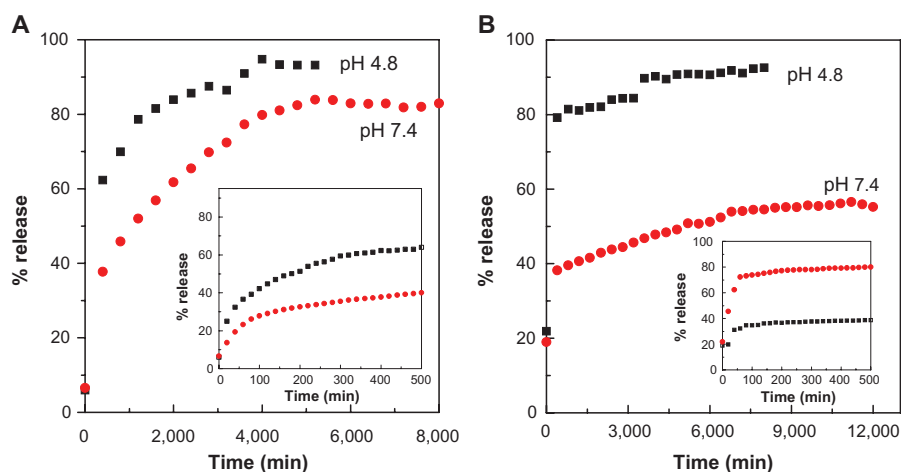


**Figure 6** Release profiles of PASA from PASA-D (A) and PASA-I (B) nanocomposites into PBS at pH 7.4 and 4.8. Insets show the release profiles of PASA from nanocomposite at initial 500 minutes time.

**Abbreviations:** PASA, para-amino salicylic acid; PASA-D, PASA nanocomposite prepared by direct method; PASA-I, PASA nanocomposite prepared by indirect method.

Using these equations for the three kinetic models, it was found that the pseudo-second-order model more satisfactorily described the kinetic release process of PASA from PASA-D and PASA-I nanocomposites. Figure 7 shows plots of the fitting of PASA released from nanocomposites.

At pH 4.8, the correlation coefficient ( $R^2$ ) was 0.9978 and 0.9991 for PASA-D and PASA-I nanocomposites, respectively, with  $k_2$  values of  $3.3 \times 10^{-5}$  and  $5.2 \times 10^{-5}$  mg/minute, respectively, and at pH 7.4, the corresponding values were 0.9946 and 0.9952, respectively, with  $k_2$  values

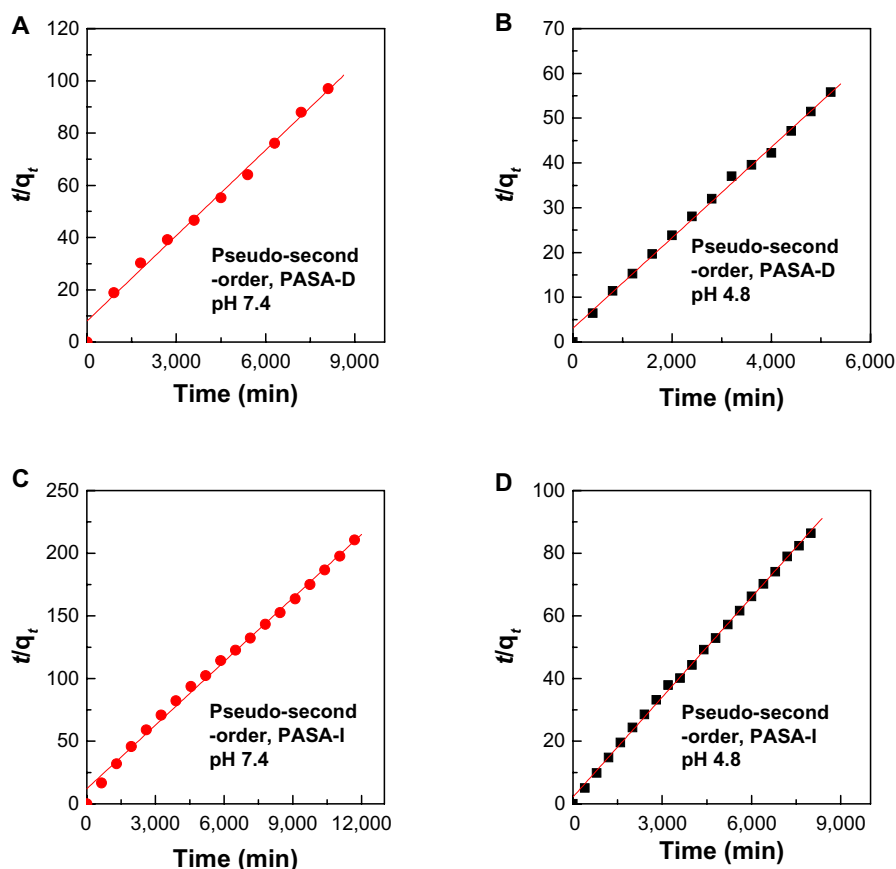


**Figure 7 (A–D)** Data fit of PASA release from PASA-D and PASA-I nanocomposites into pseudo-second-order kinetic model at pH 7.4 and 4.8.

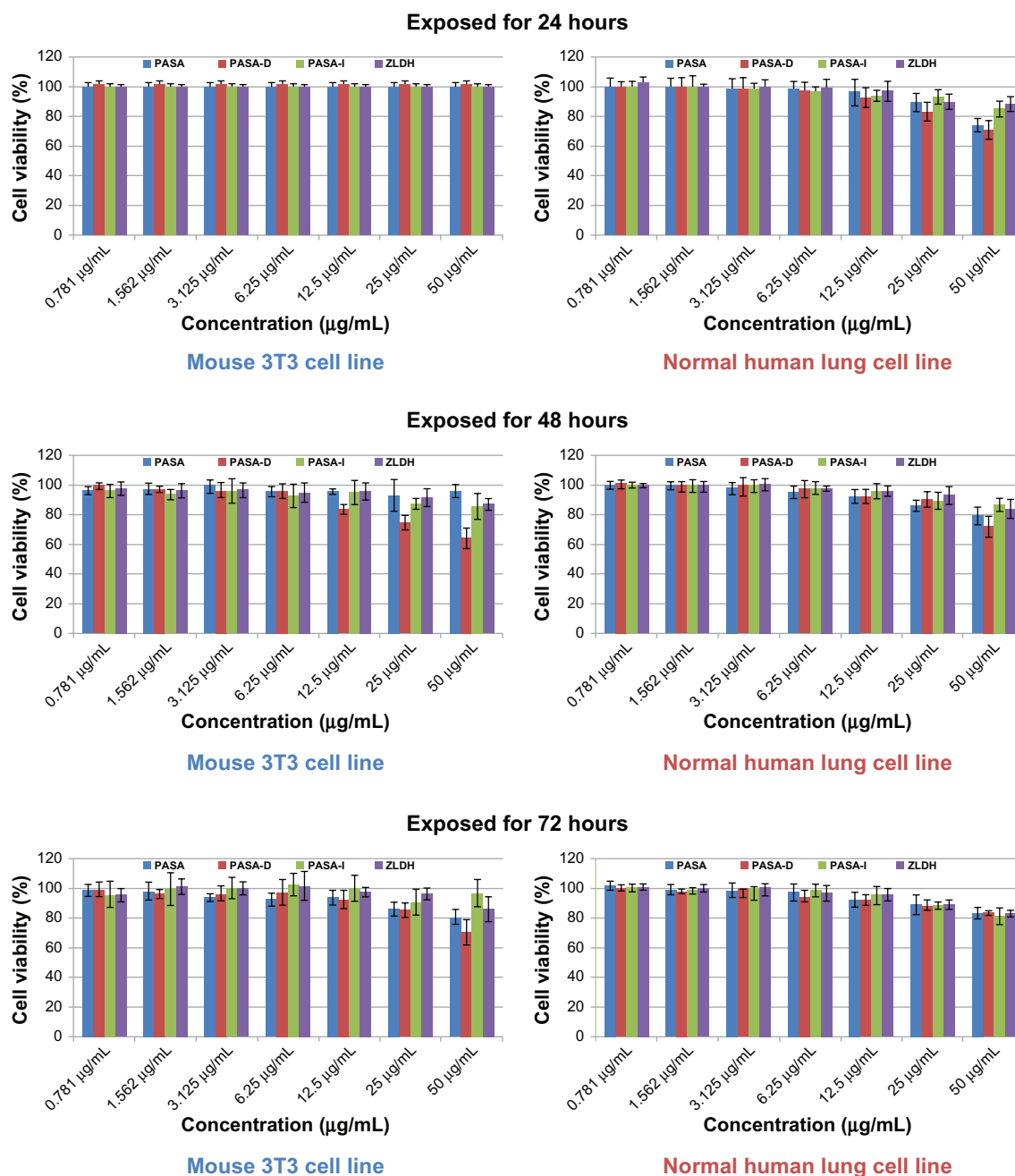
**Abbreviations:** PASA, para-amino salicylic acid; PASA-D, PASA nanocomposite prepared by direct method; PASA-I, PASA nanocomposite prepared by indirect method.



**Table 3** Correlation coefficient ( $R^2$ ), and rate constants ( $k$ ) obtained by fitting the data of PASA release from PASA-D and PASA-I nanocomposites into PBS solution at pH 4.8 and 7.4

Samples	pH	Saturation release (%)	$R^2$			Pseudo-second-order
			Pseudo-first-order	Pseudo-second-order	Parabolic diffusion model	Rate constant $k$ (mg/min)
PASA-D	7.4	88	0.8298	0.9946	0.8842	$1.5 \times 10^{-5}$
PASA-D	4.8	100	0.9129	0.9978	0.8369	$3.3 \times 10^{-5}$
PASA-I	7.4	57	0.9692	0.9952	0.9580	$1.7 \times 10^{-5}$
PASA-I	4.8	93	0.9103	0.9991	0.7849	$5.2 \times 10^{-5}$

**Abbreviations:** PASA, para-amino salicylic acid; PASA-D, PASA nanocomposite prepared by direct method; PASA-I, PASA nanocomposite prepared by indirect method; PBS, phosphate-buffered saline.

**Figure 8** Cell viability (3-[4,5-dimethylthiazol-2-yl]-2,5-diphenyltetrazolium bromide [MTT] assay) of 3T3 mouse fibroblast cells and human lung fibroblast MRC-5 cells exposed to various gradient concentrations at 24, 48, and 72 hours' exposure time. The data presented are means  $\pm$  standard deviation of triplicate samples.

**Abbreviations:** PASA, para-amino salicylic acid; PASA-D, PASA by direct method; PASA-I, PASA by indirect method; ZLDH, zinc/aluminum-layered double hydroxide.

of  $1.5 \times 10^{-5}$  and  $1.7 \times 10^{-5}$  mg/minute, respectively. All of these results are summarized in Table 3.

## Cytotoxicity study of ZLDHs and PASA, PASA-D, and PASA-I nanocomposites

In vitro toxicological studies of nanomaterials is a developing new field of research these days, aimed at understanding them and finding out their possible effects on living systems. Cell-cytotoxicity testing (MTT assay) is a very common preliminary step in assessing combustion-generated and functionalized nanoparticle-related health hazards. The MTT cytotoxicity assay reveals various cellular metabolic actions by the reduction of the yellow tetrazolium salt MTT to a purple MTT formazan. The nanocomposites PASA-D and PASA-I, at different gradient concentrations and various time points, ie, 0.781, 1.562, 3.125, 6.25, 12.5, 25, and 50  $\mu\text{g/mL}$  for 24 hours, 48 hours, and 72 hours, were exposed to 3T3 mouse fibroblast cells and human lung fibroblast MRC-5 cells. Cell viability was determined by MTT assay (Figure 8).

Neither of the PASA-D and PASA-I nanocomposites showed any reduction in cell viability during 24, 48, and 72 hours of inhibition at concentrations of 0.781–50  $\mu\text{g/mL}$ . Thus, the nanocomposite formulations possess no cytotoxicity and may be considered to be appropriate for drug-delivery purposes. Based on these preliminary toxicological findings, further detailed studies will be conducted for biomedical and translational applications.

## Conclusion

A new delivery system for PASA has been developed in this work. The drug was intercalated into ZLDH inorganic galleries by coprecipitation and ion-exchange methods. XRD, FTIR, CHNS, and TGA results indicate the successful intercalation of PASA between the LDH inorganic interlayers. The in vitro release studies show that there was a burst phenomenon occurring at the beginning of release tests at different pHs in PBS solutions, due to the absorption of the drug on the surface of ZLDH. Three kinetic models (pseudo-first-order, pseudo-second-order, and parabolic diffusion kinetic equations) were used to study the kinetics of PASA release from the nanocomposites. The kinetic studies showed the pseudo-second-order model more satisfactorily described the cumulative kinetic release process of PASA from PASA-D and PASA-I nanocomposites. The MTT results showed that the PASA-D and PASA-I nanocomposite formulations did not show any cytotoxicity against the 3T3 cell line or human lung fibroblast MRC-5 cells. All of these results suggest that ZLDH

formulations are suitable for TB chemotherapy. Therefore, we suggest that further in vivo studies should be carried out for the validation of these in vitro studies.

## Acknowledgments

Funding for this research was provided by the Ministry of Science, Technology and Innovation of Malaysia (MOSTI) under the National Nanotechnology Directorate grant NND/NA/1/TD11-010, (UPM Vot number 5489100) and the Higher Education Commission of Malaysia under the Commonwealth Scholarship and Fellowship Plan (Reference KPT.B.600-6/3, Vol 68) for Bullo Saifullah.

## Disclosure

The authors report no conflicts of interest in this work.

## References

- Duan X, Evans DG, editors. *Layered Double Hydroxides*. Heidelberg: Springer; 2006.
- Cavani F, Trifirò F, Vaccari A. Hydrotalcite-type anionic clays: preparation, properties and applications. *Catal Today*. 1991;11(2):173–301.
- Koilraj P, Thakur RS, Srinivasan K. Solid state structural transformation of tetraborate into monoborate in the interlayer galleries of reconstructed ZnAl layered double hydroxide. *J Phys Chem C*. 2013;117(13): 6578–6586.
- Kuhl S, Friedrich M, Armbruster M, Behrens M. Cu, Zn, Al layered double hydroxides as precursors for copper catalysts in methanol steam reforming-pH-controlled synthesis by microemulsion technique. *J Mater Chem*. 2012;22(19):9632–9638.
- Wang DY, Das A, Leuteritz A, et al. Structural characteristics and flammability of fire retarding EPDM/layered double hydroxide (LDH) nanocomposites. *RSC Adv*. 2012;2(9):3927–3933.
- Fu Z, Xie Y, Chen X, Jiao F, Liu L. Preparation and characteristic of chiral separation reagent pillared Zn-Al hydrotalcite-like compound. *Mater Rev*. 2010:S2.
- Hasan S, Al Ali H, Al-Qubaisi M, et al. Controlled-release formulation of antihistamine based on cetirizine zinc-layered hydroxide nanocomposites and its effect on histamine release from basophilic leukemia (RBL-2H3) cells. *Int J Nanomedicine*. 2012;7:3351–3363.
- Hussein-Al-Ali S, Al-Qubaisi M, El Zowalaty M, Hussein MZ, Ismail M. Antimicrobial activity of hippurate nanocomposite and its cytotoxicity effect in combination with cytarabine against HL-60. *J Nanomater*. 2013;2013:843647.
- Ryu SJ, Jung H, Oh JM, Lee JK, Choy JH. Layered double hydroxide as novel antibacterial drug delivery system. *J Phys Chem Solids*. 2010; 71(4):685–688.
- Hesse D, Badar M, Bleich A, et al. Layered double hydroxides as efficient drug delivery system of ciprofloxacin in the middle ear: an animal study in rabbits. *J Mater Sci Mater Med*. 2013;24(1):129–136.
- Saifullah B, Hussein MZ, Hussein Al Ali SH. Controlled-release approaches towards the chemotherapy of tuberculosis. *Int J Nanomedicine*. 2012;7:5451.
- World Health Organization. *Global Tuberculosis Report 2012*. Geneva: WHO; 2012.
- Mitchison DA. Role of individual drugs in the chemotherapy of tuberculosis. *Int J Tuberc Lung Dis*. 2000;4(9):796–806.
- Mitnick C, Bayona J, Palacios E, et al. Community-based therapy for multidrug-resistant tuberculosis in Lima, Peru. *N Engl J Med*. 2003;348(2):119–128.
- Crepaldi EL, Pavan PC, Valim JB. Comparative study of the coprecipitation methods for the preparation of layered double hydroxides. *J Braz Chem Soc*. 2000;11(1):64–70.

16. Lakraimi M, Legrouri A, Barroug A, De Roy A, Besse JP. Preparation of a new stable hybrid material by chloride-2,4-dichlorophenoxyacetate ion exchange into the zinc-aluminium-chloride layered double hydroxide. *J Mater Chem*. 2000;10(4):1007-1011.
17. Rives V. *Layered Double Hydroxides: Present and Future*. Hauppauge (NY): Nova Science; 2001.
18. Hussein-Al-Ali SH, Al-Qubaisi M, Hussein MZ, Ismail M, Zainal Z, Hakim MN. In vitro inhibition of histamine release behavior of cetirizine intercalated into Zn/Al- and Mg/Al-layered double hydroxides. *Int J Mol Sci*. 2012;13(5):5899-5916.
19. Oriakhi CO, Farr IV, Lerner MM. Incorporation of poly(acrylic acid), poly(vinylsulfonate) and poly(styrenesulfonate) within layered double hydroxides. *J Mater Chem*. 1996;6(1):103-107.
20. Crepaldi EL, Pavan PC, Valim JB. Anion exchange in layered double hydroxides by surfactant salt formation. *J Mater Chem*. 2000;10(6):1337-1343.
21. Newman SP, Williams SJ, Coveney PV, Jones W. Interlayer arrangement of hydrated MgAl layered double hydroxides containing guest terephthalate anions: comparison of simulation and measurement. *J Phys Chem B*. 1998;102(35):6710-6719.
22. Akkaya Y, Akyuz S. Infrared and Raman spectra, ab initio calculations vibrational assignment of 4-aminosalicylic acid. *Vib Spectrosc*. 2006;42(2):292-301.
23. Li F, Zhang L, Evans DG, Forano C, Duan X. Structure and thermal evolution of Mg-Al layered double hydroxide containing interlayer organic glyphosate anions. *Thermochim Acta*. 2004;424(1-2):15-23.
24. Panicker CY, Varghese HT, John A, Philip D, Istvan K, Keresztury G. FT-IR, FT-Raman and FT-SERS spectra of 4-aminosalicylic acid sodium salt dihydrate. *Spectrochim Acta A Mol Biomol Spectrosc*. 2002;58(2):281-287.
25. Silion M, Hritcu D, Popa MI. Intercalation of salicylic acid into ZnAl layered double hydroxides by ion-exchange and coprecipitation method. *J Optoelectron Adv Mater*. 2009;11(4):528-534.
26. Klopogge JT, Frost RL. Fourier transform infrared and Raman spectroscopic study of the local structure of Mg-, Ni-, and Co-hydrated cations. *J Solid State Chem*. 1999;146(2):506-515.
27. Rotich MK, Brown ME, Glass BD. Thermal studies on mixtures of aminosalicylic acids with cyclodextrins. *J Therm Anal Calorim*. 2003;73(2):687-706.
28. Cheng X, Huang X, Wang X, Sun D. Influence of calcination on the adsorptive removal of phosphate by Zn-Al layered double hydroxides from excess sludge liquor. *J Hazard Mater*. 2010;177(1):516-523.
29. Huang X, Brazel CS. On the importance and mechanisms of burst release in matrix-controlled drug delivery systems. *J Control Release*. 2001;73(2):121-136.
30. Khan AI, O'Hare D. Intercalation chemistry of layered double hydroxides: recent developments and applications. *J Mater Chem*. 2002;12(11):3191-3198.
31. bin Hussein MZ, Zainal Z, Yahaya AH, Foo DWV. Controlled release of a plant growth regulator, alpha-naphthaleneacetate from the lamella of Zn-Al-layered double hydroxide nanocomposite. *J Control Release*. 2002;82(2):417-427.
32. Zhang H, Zou K, Sun H, Duan X. A magnetic organic-inorganic composite: synthesis and characterization of magnetic 5-aminosalicylic acid intercalated layered double hydroxides. *J Solid State Chem*. 2005;178(11):3485-3493.
33. Fogg AM, Dunn JS, Shyu SG, Cary DR, O'Hare D. Selective ion-exchange intercalation of isomeric dicarboxylate anions into the layered double hydroxide  $[\text{LiAl}_2(\text{OH})_6]\text{Cl}\cdot\text{H}_2\text{O}$ . *Chem Mater*. 1998;10(1):351-355.
34. Fogg AM, Dunn JS, O'Hare D. Formation of second-stage intermediates in anion-exchange intercalation reactions of the layered double hydroxide  $[\text{LiAl}_2(\text{OH})_6]\text{Cl}\cdot\text{H}_2\text{O}$  as observed by time-resolved, in situ X-ray diffraction. *Chem Mater*. 1998;10(1):356-360.
35. Dong L, Yan L, Hou WG, Liu SJ. Synthesis and release behavior of composites of camptothecin and layered double hydroxide. *J Solid State Chem*. 2010;183(8):1811-1816.
36. Ho YS, Ofomaja AE. Pseudo-second-order model for lead ion sorption from aqueous solutions onto palm kernel fiber. *J Hazard Mater*. 2006;129(1):137-142.
37. Kong X, Shi S, Han J, Zhu F, Wei M, Duan X. Preparation of glycyl-L-tyrosine intercalated layered double hydroxide film and its in vitro release behavior. *Chem Eng J*. 2010;157(2):598-604.

## Drug Design, Development and Therapy

### Publish your work in this journal

Drug Design, Development and Therapy is an international, peer-reviewed open-access journal that spans the spectrum of drug design and development through to clinical applications. Clinical outcomes, patient safety, and programs for the development and effective, safe, and sustained use of medicines are a feature of the journal, which

Submit your manuscript here: <http://www.dovepress.com/drug-design-development-and-therapy-journal>

Dovepress

has also been accepted for indexing on PubMed Central. The manuscript management system is completely online and includes a very quick and fair peer-review system, which is all easy to use. Visit <http://www.dovepress.com/testimonials.php> to read real quotes from published authors.